A STUDY OF MHD FLUID WITH SECOND ORDER SLIP AND THERMAL FLOW OVER A NONLINEAR STRETCHING SHEET

Shefali JAUHRI[*]
Department of Mathematics, Jaipur National University, Agra Bypass, Near New RTO Office
Jagatpura, 302017 Jaipur, INDIA
E-mail: shefali.jauhri3@gmail.com

Upendra MISHRA
Department of Mathematics, Amity University Rajasthan, NH-11 C
Kant Kalwar, Delhi-Jaipur Highway, Near Achrol Village, Jaipur, INDIA

An electrically conducted viscous incompressible nanofluid flow caused by the nonlinear stretching surface with stagnation flow has been investigated numerically. The effect of Brownian motion and thermophoresis on the nanofluid is also incorporated. The governing partial differential equations with nonlinear second order boundary conditions are solved by the fourth order Runge-Kutta technique using MATLAB programming. The effect of the radiation parameter (R_d), stretching parameter (n), Brownian motion parameter (N_b), thermophoresis parameter (N_t) on temperature, velocity and mass transfer are shown graphically. The influence of some of these parameters on the local Nusselt number ($-\theta'(0)$) and local Sherwood number ($-\phi'(0)$) are shown by the graphs.

Keywords: stagnation point flow, second order slip boundary conditions, nonlinear stretching sheet, Runge-Kutta method.

1. Introduction

In recent years, the investigation of flow with nonlinear stretching surfaces and magneto-nanofluids has produced benefits due to its various mechanical applications. It is used in a lot of modern fields, such as polymer fibre creation, milling, metalworking, etc. The boundary layer and flow problems are turning into an extremely noticeable area of research and analysis.

Ahmed [1] worked on a Walter's Model-B fluid in a boundary layer flow over a stretching plate. He solved the problem of heat transfer with variable thermal conductivity in two different parts: first, the prescribed surface temperature and second, the prescribed stretching plate heat flux. Ahmed [2] discussed the boundary layer flow of a viscous incompressible fluid over a stretching plate. He explained the effect of the suction parameter with variable thermal conductivity on the temperature field in two different parts: first, the prescribed surface temperature and second, the prescribed stretching plate heat flux. Anderson [3] studied the viscoelastic fluid flow across a transverse magnetic field on a stretching surface and obtained the exact analytic solution for the boundary layer.

Bentwhich [4] explored and found a solution to a two-dimensional problem with the help of an Oseen equation and Reynolds number. Bhargava *et al.* [5] studied a micropolar flow over a nonlinear stretching sheet. Chen [6] discussed the laminar boundary layer flow on a stretching sheet with the consideration of two cases: first, the sheet with recommended wall temperature and second, with heat transfer on a continuous surface. Choi [7] was the first to use a nanofluid by adding nanoscale particles.

Cortell [8] examined a viscous fluid flow over a nonlinear stretching sheet by analysing two cases: CST and PST. Crane [9] was the first to solve two-dimensional Navier-Stokes equations. He examined the time-independent, two-dimensional incompressible boundary layer flow of a Newtonian fluid on a stretching flat plate moving in its plane with variable direct velocity under the fixed point with uniform pressure.

---

[*] To whom correspondence should be addressed

Fang [10] discussed the magnetohydrodynamic (MHD) flow over a linearly stretching surface in a porous medium with slip conditions. Hayat [11] discussed the magnetohydrodynamic (MHD) flow of Jeffrey liquid along with a nonlinear radially stretched sheet. Heat transfer is characterized by Newtonian and Joule heating effects. Hasio [12] investigated the nanofluid energy conversion problem with slip boundary conditions on stretching sheets and explained the application of the applied energy effect in the aspect of heat and mass transfer.

Kalidas [13] investigated the effect of a magnetohydrodynamic (MHD) mixed convection flow of stagnation-point over a nonlinear surface with slip velocity and controlled surface temperature. Kang *et al.* [14] carried out mathematical and exploratory examinations on the thermal conductivity of nanofluids. To improve the conductivity of thermal nanofluids, he used the volume of nanoparticles rather than the volume of the fluid. Khan and Pop [15] worked numerically on stretching surfaces in a nanofluid with laminar flow.

Nandeppanavar *et al.* [16] considered the second-order slip boundary condition and investigated the consequences of heat transfer effects with PST and PHF heating process. Nagendramma [17] examined a two-dimensional triple-diffusive boundary layer slip parameter of a nanofluid over a nonlinear stretching surface immersed in a porous medium. The utilized model for the nanofluid consolidates the impacts of thermophoresis, Brownian motion, cross-dispersion, and the power-law extending boundary. Rosca *et al.* [18] investigated the boundary layer under the condition of zero velocity point flow and discussed the effect of second-order slip velocity over a nonlinear stretching/shrinking sheet.

Sakiadis [19] discussed the boundary layer behavior on continuous solid surfaces with arrangements of the surfaces differing significantly from those for boundary layer flow on surfaces of limited length. Seth [20] explored the stagnation point flow of nanofluids in the direction of a nonlinearly stretching sheet of variable thickness in the presence of an electromagnetic field and convective heating. The novel idea of non-radiative heat transfer is likewise considered. The nanofluid is propelled by the Lorentz force which arises from the attraction of electric and magnetic fields. Likewise, the effect of physical limits is considered and presented in graphs and tables. Shen [21] analyzed the time-independent boundary layer flow over an impermeable moving vertical flat plate with the convection boundary condition at the left half of the flat plate. He shows that a similar arrangement is possible if the convection boundary condition in heat transfer is connected with the heated or cooled liquid on the left half of the flat plate. Likewise, the effects of the boundary conditions on skin friction, heat transfer, divider temperature, and velocity and temperature profiles are investigated on the streamlines and isotherms.

Siddappa [22] explored Crane's flow issue to the viscoelastic fluid of Walter's Model-B fluid. Subhas [23] discussed the viscoelastic fluid flow and heat transfer characteristics in a saturated porous medium. He considered PHF and PST cases and determined the velocity field and skin friction. Wang [23] extended Crane's paper. He worked on the three-dimensional boundary flow on a flat stretching sheet and found the exact solution of the Navier-Stokes equation.

We aim to focus on the effect of the radiation parameter (Rd), stretching parameter (n), Brownian motion parameter (Nb), and thermophoresis parameter (Nt) in the presence of second-order velocity parameters on stagnation flow over a nonlinearly stretching sheet with mixed convection heat and mass transfer with electrical magnetohydrodynamics.

2. Mathematically formulation

In this paper, we consider a steady, electrically conducting viscous incompressible, two-dimensional nano-fluid stagnation flow with second-order slip boundary conditions. The heat transfer with electric and magnetic effects under mixed convection is also considered. The stagnation flow is taken into account through an infinite vertical sheet. The stream of the fluid is heading along with the sheet, on which the x-direction is considered as tangent and the y-direction as normal. Therefore, the flow is stagnation flow. A schematic representation of the physical model and coordinates system is represented in Fig. 1.

The governing equations are

$$\frac{\partial u}{\partial x} + \frac{\partial v}{\partial y} = 0 \,, \tag{2.1}$$

$$u\frac{\partial u}{\partial x}+v\frac{\partial u}{\partial y}=u_{\infty}\frac{\partial u_{\infty}}{\partial x}+\nu_f\frac{\partial^2 u}{\partial y^2}-\sigma\frac{B_0^2}{\rho_f}u++g_x\beta_t\left(T-T_{\infty}\right)+g_x\beta_c\left(C-C_{\infty}\right),\qquad(2.2)$$

$$u\frac{\partial T}{\partial x}+v\frac{\partial T}{\partial y}=\frac{K_f}{(\rho c_p)_f}\frac{\partial^2 T}{\partial y^2}+\frac{Q_0}{(\rho c_p)_f}\left(T-T_{\infty}\right)+$$

$$+\frac{(\rho c_p)_p}{(\rho c_p)_f}\left[D_B\frac{\partial C}{\partial y}\frac{\partial T}{\partial y}+\frac{D_T}{T_{\infty}}\left(\frac{\partial T}{\partial y}\right)^2\right]+\frac{\nu}{c_p}\left(\frac{\partial u}{\partial y}\right)^2-\frac{1}{(\rho c)_f}\frac{\partial q_r}{\partial y},\qquad(2.3)$$

$$u\frac{\partial C}{\partial x}+v\frac{\partial C}{\partial y}=D_B\frac{\partial^2 C}{\partial y^2}+\frac{D_T}{T_{\infty}}\frac{\partial^2 T}{\partial y^2}\;.\qquad(2.4)$$
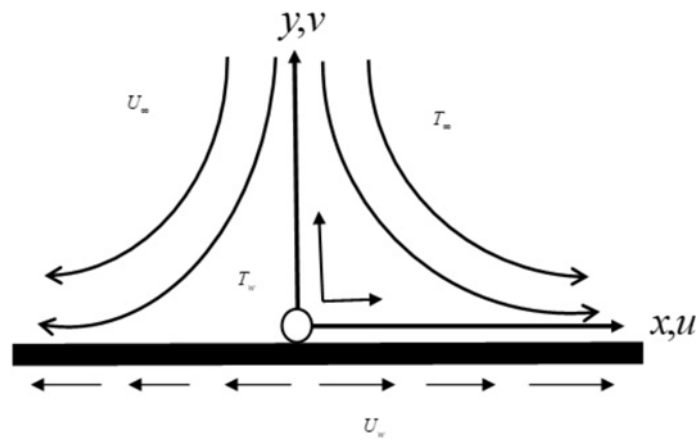
Fig.1. Physical model and coordinates system.

The boundary-conditions are

$$\left.\begin{array}{l}u=ax^n+N_1\dfrac{\partial u}{\partial y}+N_2\dfrac{\partial^2 u}{\partial y^2},v=0\\[2mm]T=T_W+K_T\dfrac{\partial T}{\partial y}\\[2mm]C=C_W+K_C\dfrac{\partial C}{\partial y}\end{array}\right\}\qquad\text{as}\quad y=0,\qquad(2.5)$$

$$\left.\begin{array}{l}u\to 0\\ T\to T_{\infty}\\ C\to C_{\infty}\end{array}\right\}\qquad\text{as}\qquad y\to\infty\;.\qquad(2.6)$$

Here, u (along the x-axis) and v (along the y-axis) are velocity components, (α_m) is the thermal diffusivity, (υ) is the kinematic viscosity, 'a' is a positive constant, (D_B) is the Brownian diffusion

coefficient, (D_T) is the thermophoretic diffusion coefficient and the stress parameter $\tau = \dfrac{(\rho c_p)_p}{(\rho c_p)_f}$ is the ratio

between the effective heat capacity of the nanoparticle material and heat capacity of the fluid.

We are looking for similarity solution of Eqs (2.1)-(2.4) with boundary conditions (2.5)-(2.6).

$$u = ax^n f'(\eta) \quad \text{and} \quad v = -\left(\sqrt{\frac{a\nu(n+1)}{2}}\right) \cdot x^{\left(\frac{n-1}{2}\right)} \left[f(\eta) + \left(\frac{n-1}{n+1}\right) \eta f'(\eta) \right] \tag{2.7}$$

To solve equations

$$\eta = y\sqrt{\frac{a(n+1)}{2}} x^{\left(\frac{n-1}{2}\right)}, \qquad \theta(\eta) = \frac{T - T_\infty}{T_W - T_\infty}, \tag{2.8}$$

$$\Psi = \sqrt{\frac{2a\nu}{(n+1)}} \, x^{\left(\frac{n+1}{2}\right)} f(\eta). $$

We use equation (2.7) and (2.8) in Eqs (2.2)-(2.4). The following differential equations are obtained,

$$f''' + ff'' + \left(\frac{2n}{n+1}\right)\left[1 - f'^2\right] - Mf' + G_t\theta + G_c\phi = 0, \tag{2.9}$$

$$\left(\frac{1}{Pr} + Rd\right)\theta'' + f\theta' + \lambda\theta + N_b\theta'\phi' + N_t\theta'^2 + Ecf''^2 = 0, \tag{2.10}$$

$$\phi'' + Lef\phi' + \frac{N_t}{N_b}\theta'' = 0. \tag{2.11}$$

Here $Pr = \dfrac{\nu_f}{\alpha}$ is the Prandtl number, $M = \dfrac{\sigma B_0^2}{a\rho_f}$ is nondimensional magnetic parameter.

The boundary conditions are

$$f(0) = 0, f'(0) = 1 + L_1 f''(0) + L_2 f'''(0),$$

$$\theta(0) = 1 + \delta_1\theta'(0), \qquad \text{at} \quad \eta = 0, \tag{2.12}$$

$$\phi(0) = 1 + \delta_2\phi'(0),$$

$$\left.\begin{array}{l} f' \to 0 \\[4pt] \theta \to 0 \\[4pt] \phi \to 0 \end{array}\right\} \quad \text{as} \quad \eta \to \infty. \tag{2.13}$$

Here $L_I = N_I \sqrt{\dfrac{a}{\nu_f}}$, $\delta_I = k_T \sqrt{\dfrac{a}{\nu_f}}$, $\delta_2 = k_C \sqrt{\dfrac{a}{\nu_f}}$ are nondimensional slip parameters.

2.1. Nusselt number

The Nusselt number explains the difference of heat transfer through a liquid layer because of convection comparative with conduction over a similar fluid layer. The Nusselt number can be defined as

$$Nu = \frac{xq_w}{k(T_w - T_\infty)}.$$

2.2. Sherwood number

The Sherwood number is utilized in mass transfer. Additionally, it is called a Nusselt number in mass transfer. It conveys the proportion of the convective mass exchange to the rate of diffusive mass transport. The Sherwood number can be defined as

$$Sh = \frac{xq_m}{D_B(C_w - C_\infty)}$$

where $\tau_w = \mu\left(\dfrac{\partial u}{\partial y}\right)$ is the tangential stress along the plate, $q_w = -k\left(\dfrac{\partial T}{\partial y}\right)$ at $y = 0$ is the wall heat, q_m is the mass flux, k is the coefficient of thermal conductivity, x is the characteristic length.

Let us introduce the following parameters: $Re_x = \dfrac{u_w x}{\upsilon}$ is known as the local Reynolds number. $\dfrac{Nu}{Re_x^{1/2}} = -\theta'(0)$ and $\dfrac{Sh}{Re_x^{1/2}} = -\phi'(0)$ as the reduced Nusselt number and reduced Sherwood number, respectively. The local skin friction C_f can be defined as

$$C_f = \frac{\tau_w}{\rho u_e^2(x)}. \tag{2.14}$$

Using Eqs (2.8), (2.12) and (2.13), we get

$$(Re)^{-\left(\frac{1}{2}\right)} Nu_x = \sqrt{\frac{(n+1)}{2}}\left[-\theta'(0)\right], \qquad \sqrt{Re}\; C_f = \sqrt{\frac{(n+1)}{2}} f''(0).$$

3. Result and discussion

The changed momentum, temperature, and concentration Eqs (2.9)-(2.11) with boundary conditions (2.12) and (2.13) were numerically solved by utilizing the Runge-Kutta fourth order strategy alongside the shooting method. We acquired velocity, temperature profile graphs for various parameters.

Table 1. Comparison of $-\theta'(0)$ and $-\phi'(0)$ for various values of parameters N_t and N_b when $S_0 = G_t = G_c = K_1 = L_1 = \delta_1 = \delta_2 = \lambda = R_d = M = E = S = 0$, $Sc = Pr = 10$ and $n = 1$. The result is validated with the results obtained by Khan and Pop [14].

N_t	N_b	$-\theta'(0)$ Khan and Pop	$-\phi'(0)$ Khan and Pop	$-\theta'(0)$ Present Result	$-\phi'(0)$ Present Result
0.1	0.1	0.9524	2.1294	0.9524	2.1293
0.2	0.2	0.3654	2.5152	0.3654	2.5151
0.3	0.3	0.1355	2.6088	0.1355	2.6087
0.4	0.4	0.0495	2.6038	0.0495	2.6037
0.5	0.5	0.0179	2.5731	0.0179	2.5730

The mixed convection issue related to a time-independent, non-linear, two-dimensional stagnation point nanofluid flow over a stretching surface is also examined and numerical outcomes are obtained. The BLP defined is changed into an IVP by shooting strategy as the analytic strategies fail to understand the arrangement of different conditions together. The outcomes acquired are shown through the graphs for temperature, velocity, and concentration profile as well as the local Nusselt, and Sherwood number, respectively. To analyse the results, a numerical computation effort has been undertaken using the procedure characterized above. To study the outcomes, a numerical calculation has been done by utilizing the Runge Kutta fourth-order technique followed by a shooting strategy.

Effect of magnetic field parameter

Figures 2 to 6 represent the effect of the magnetic parameter M on the non-dimensional velocity, temperature, concentration profile, local Nusselt, and Sherwood number.
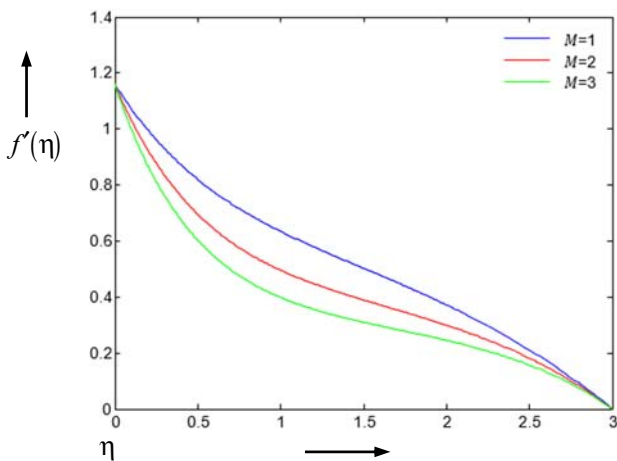
Fig.2. Effect of different values of magnetic parameter M versus η on $f'(\eta)$ with $Pr = 10$, $n = 1$, $N_t = 0.1$, $N_b = 0.1$, $Gt = 0.1$, $Gc = 0.1$, $R_d = 0.1$, $Ec = 0.1$, $E = 0.1$, $\lambda = 0.1$, $L_2 = 0.1$.
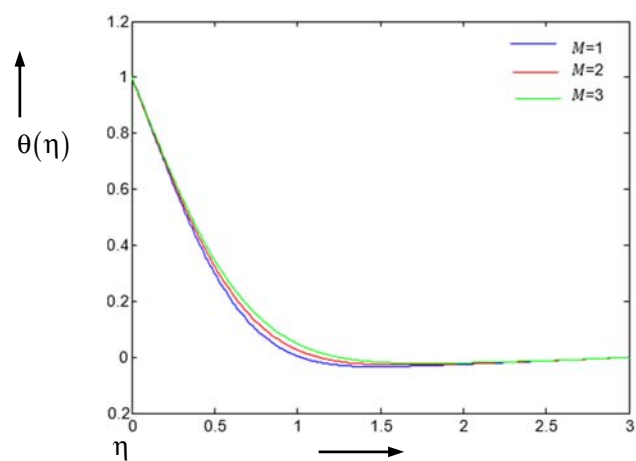
Fig.3. Effect of different values of magnetic parameter M versus η on $\theta(\eta)$ with $Pr = 10$, $n = 1$, $N_t = 0.1$, $N_b = 0.1$, $Gt = 0.1$, $Gc = 0.1$, $R_d = 0.1$, $Ec = 0.1$, $E = 0.1$, $\lambda = 0.1$, $L_2 = 0.1$.

On increasing the value of *M* and keeping the other parameters constant, the temperature, concentration, and Sherwood number are increasing while fluid velocity and Nusselt number are decreasing. On increasing *M*, the Lorentz force developed, which opposes the motion of the fluid, and therefore the momentum boundary layer reduces while the thermal boundary layer increases. Hence, velocity decreases (as shown in Fig.2) and temperature increases (as shown in Fig.3). We found that near the surface of the sheet, the concentration profile increases while at some distance from the wall the concentration profile decreases.
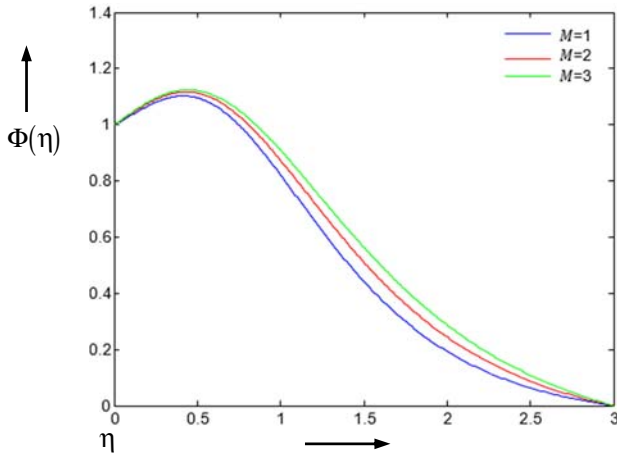
Fig.4. Effect of different values of magnetic parameter *M* on $\Phi(\eta)$.
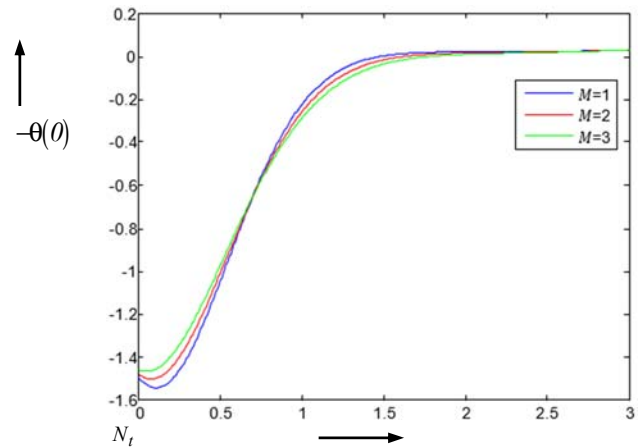
Fig.5. Effect of different values of magnetic parameter *M* on $-\theta'(0)$.
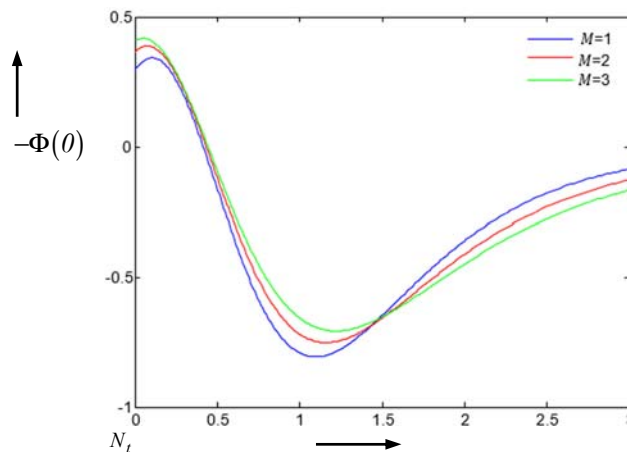
Fig.6. Effect of different values of magnetic parameter *M* on $-\Phi'(0)$.

Effect of radiation parameter

Figures 7 to 9 represent the effect of the radiation parameter R_d on the non-dimensional velocity, temperature, concentration profile. On increasing the value of R_d and keeping other parameters constant, the velocity and temperature profile increase while the concentration profile decreases. An increment in the radiation parameter means an increment in the external thermal energy which is the reason of an increment in temperature. The concentration of nanofluid increases near the plate and decreases away from the wall.
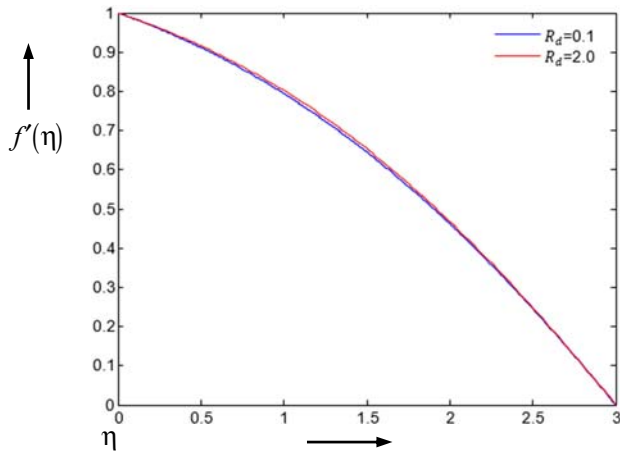
Fig.7. Effect of different values of radiation parameter R_d on $f'(\eta)$.
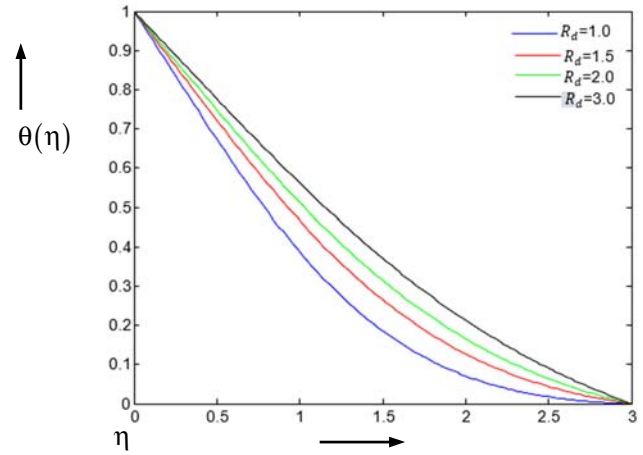
Fig.8. Effect of different values of radiation parameter R_d on $\theta(\eta)$.
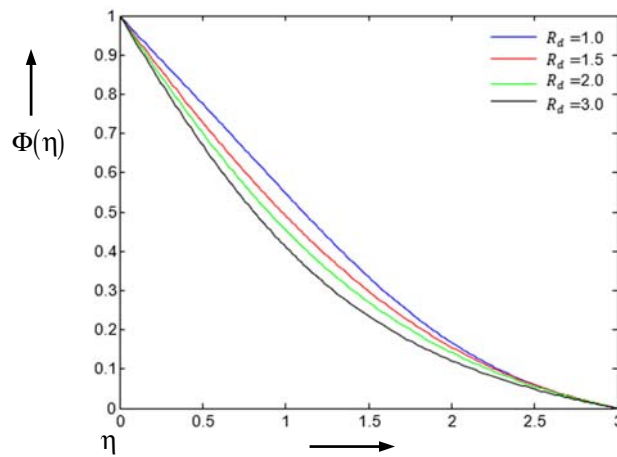
Fig.9. Effect of different values of radiation parameter R_d on $\Phi(\eta)$.

Effect of nonlinear parameter

Figures 10 to 14 represent the effect of the nonlinear parameter n on the non-dimensional velocity, temperature, concentration profile, local Nusselt, and Sherwood number. On increasing the value of n and keeping other parameters constant, the temperature and concentration profile decrease while the fluid velocity, Nusselt number, and Sherwood number increase.
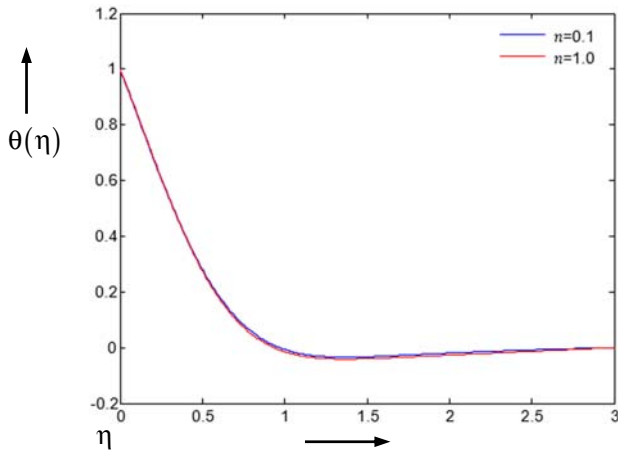
Fig.10. Effect of different values of nonlinear parameter n on $\theta(\eta)$.
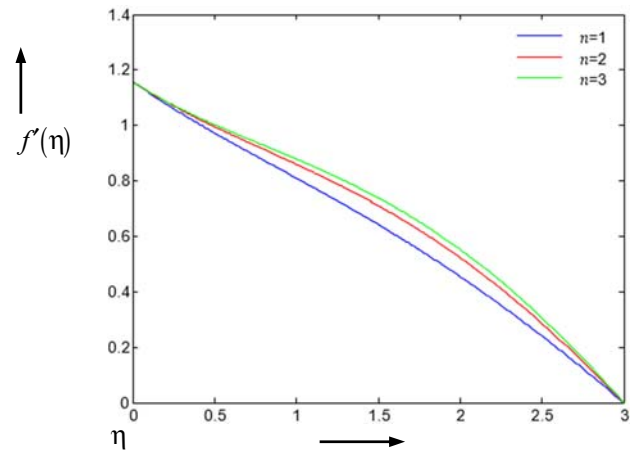
Fig.11. Effect of different values of nonlinear parameter n on $f'(\eta)$.
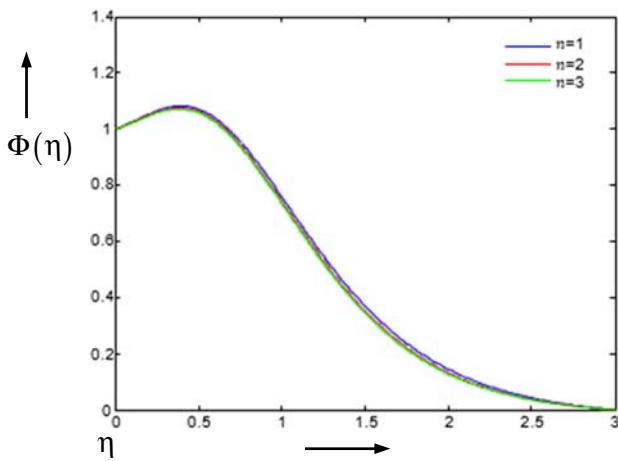
Fig.12. Effect of different values of nonlinear parameter n versus η on $f'(\eta)$.
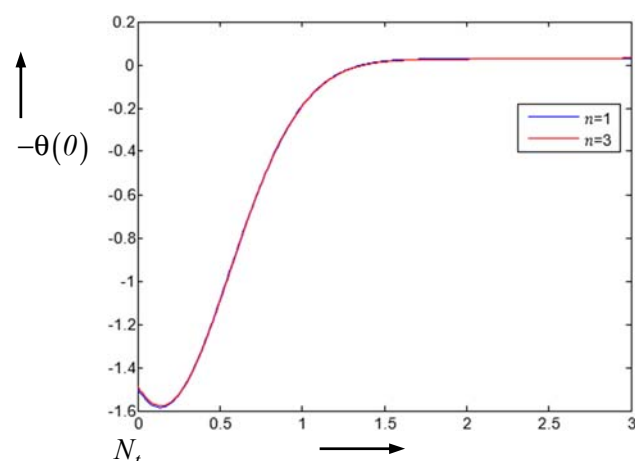
Fig.13. Effect of different values of nonlinear parameter n versus N_t on $-\theta'(\eta)$.
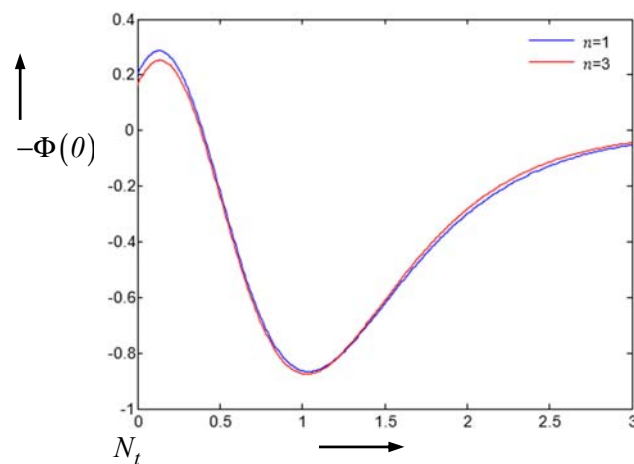
Fig.14. Effect of different values of nonlinear parameter n on $-\Phi'(0)$.

Effect of second order velocity slip parameter

      The impact of the second-order velocity slip parameter L_2 on the non-dimensional velocity, temperature, concentration profile, and local Nusselt and Sherwood number is illustrated in Figs 15-19. On increasing the value of L_2 and keeping other parameters constant, the momentum boundary layer increases while the thermal boundary layer decreases. Hence temperature, concentration, and Nusselt number decrease while the fluid velocity and Sherwood number increase.
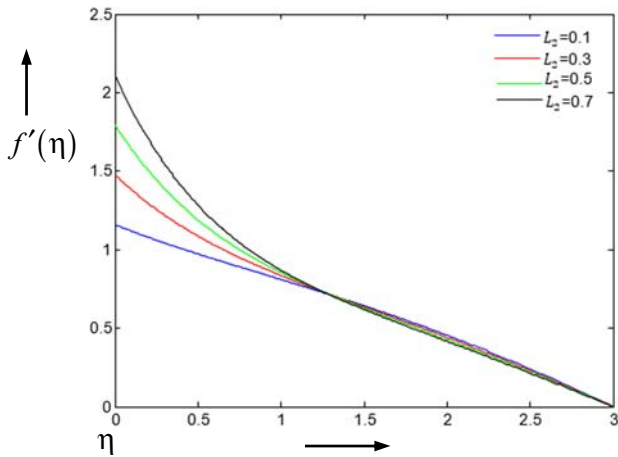
Fig.15. Effect of different values of second order slip velocity parameter L_2 on $f'(\eta)$.
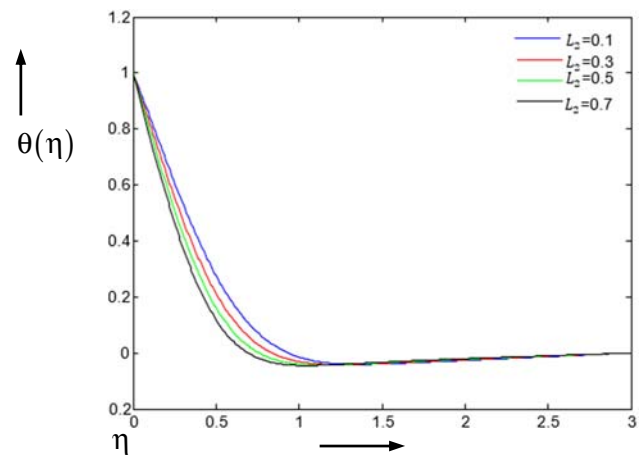
Fig.16. Effect of different values of second order slip velocity parameter L_2 on $\theta(\eta)$.
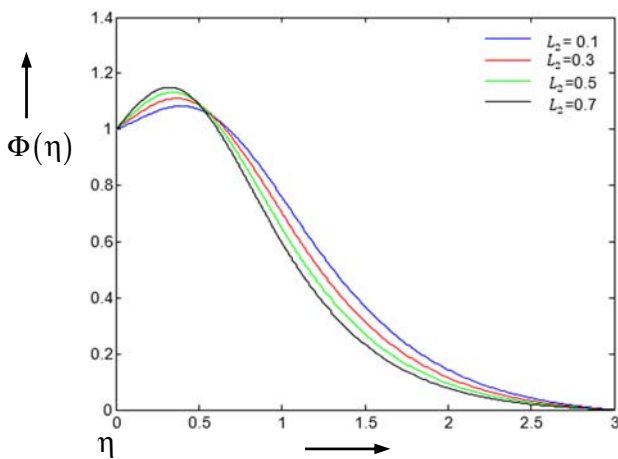
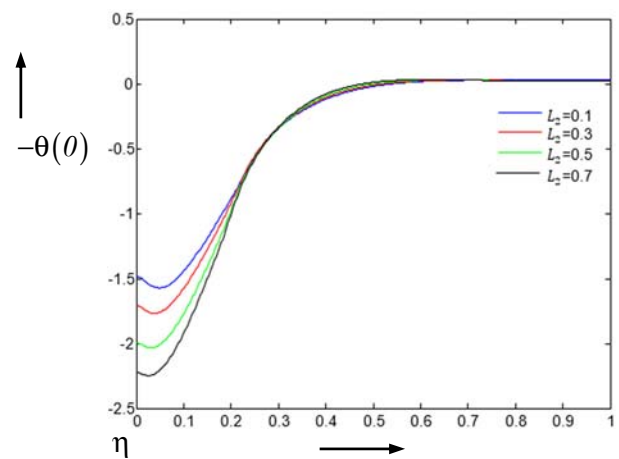Fig.17. Effect of different values of second order slip velocity parameter L_2 on $\Phi(\eta)$.

Fig.18. Effect of different values of second order slip velocity parameter L_2 on $-\theta'(0)$.
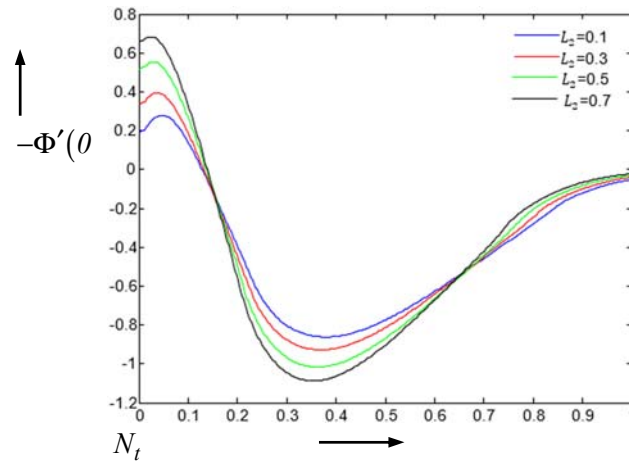
Fig.19. Effect of different values of second order slip velocity parameter L_2 on $-\Phi'(0)$.

Effect of thermophoresis parameter and Brownian motion parameter

Figures 20 to 24 represent the effect of the thermophoresis parameter N_t and the Brownian motion parameter N_b simultaneously on the non-dimensional velocity, temperature, concentration, local Nusselt, and Sherwood number.

On increasing the value of N_t and N_b and keeping other parameters constant, the thermal boundary layer decreases, and hence the temperature, concentration profile, Sherwood number decrease while the momentum boundary layer increases so the fluid velocity and Nusselt number increase.
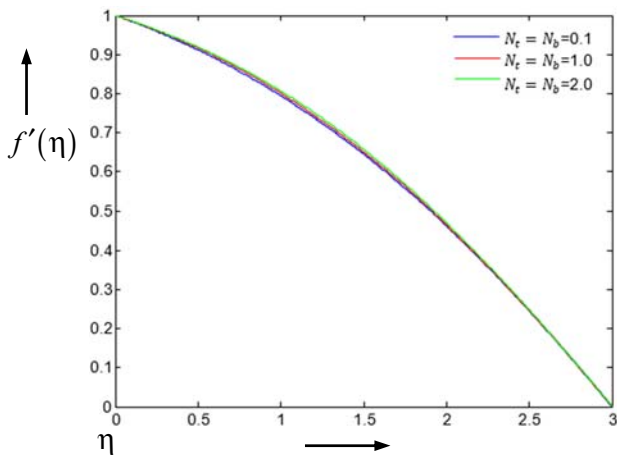

Fig.20. Effect of different values of Brownian motion and thermophoresis parameter N_t and N_b on $f'(\eta)$.
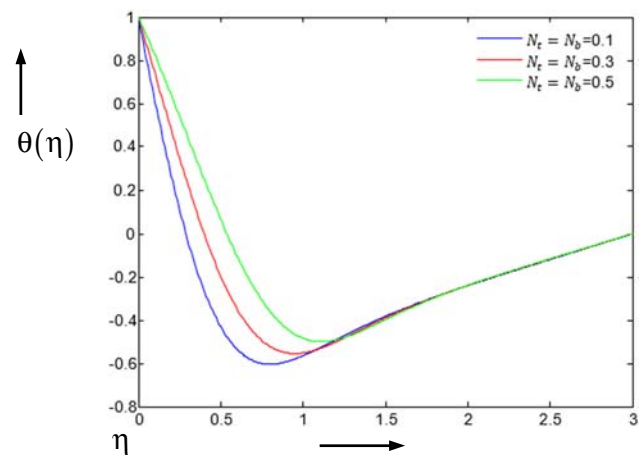

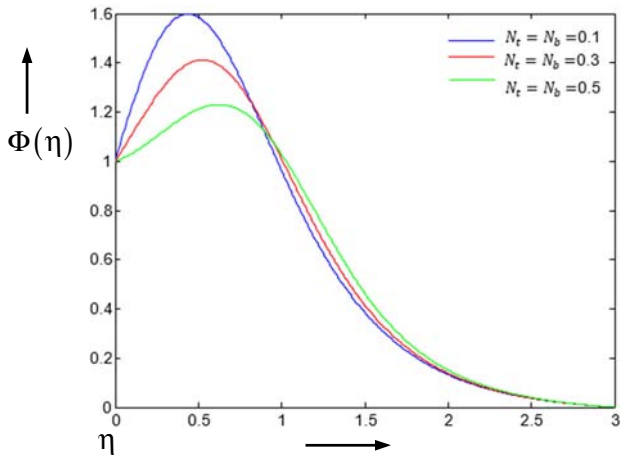Fig.21. Effect of different values of Brownian motion and thermophoresis parameter N_t and N_b on $\theta(\eta)$.

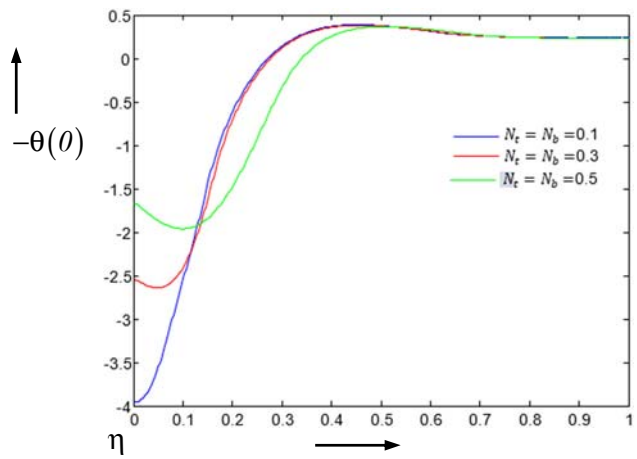Fig.22. Effect of different values of Brownian motion and thermophoresis parameter N_t and N_b on $\Phi(\eta)$.

Fig.23. Effect of different values of Brownian motion and thermophoresis parameter N_t and N_b versus η on $-\theta'(0)$.
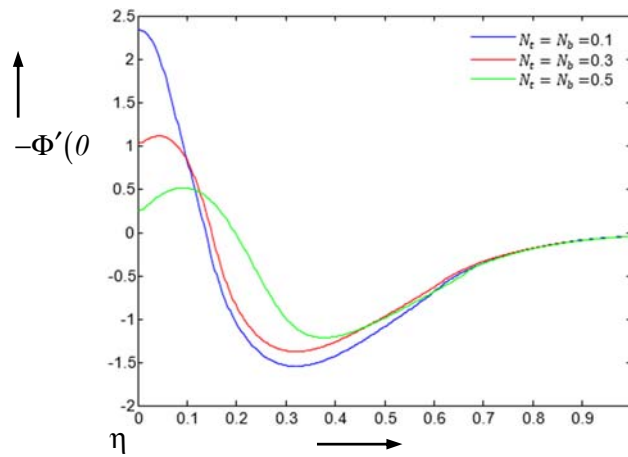

Fig.24. Effect of different values of Brownian motion and thermophoresis parameter N_t and N_b on $-\Phi'(0)$.

Effect of stretching/shrinking parameter

Figures 25 to 29 represent the effect of the stretching parameter $\lambda > 0$ on the non-dimensional velocity, temperature, concentration profile, and local Nusselt and Sherwood number. On increasing the value of $\lambda > 0$ and keeping other parameters constant, the thermal boundary layer and momentum boundary layer both decrease hence the temperature, concentration profile, Sherwood number, fluid momentum, and Nusselt number decrease.
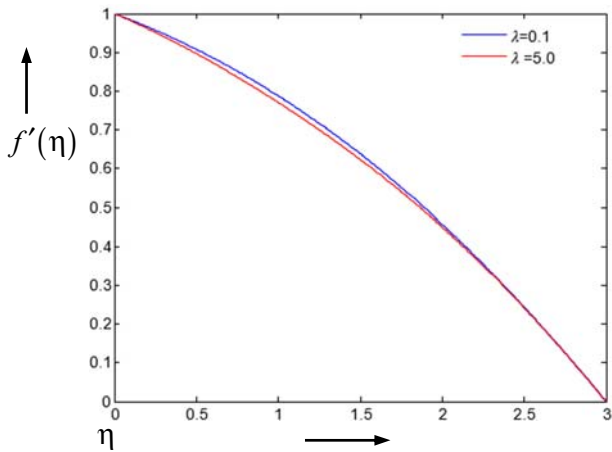
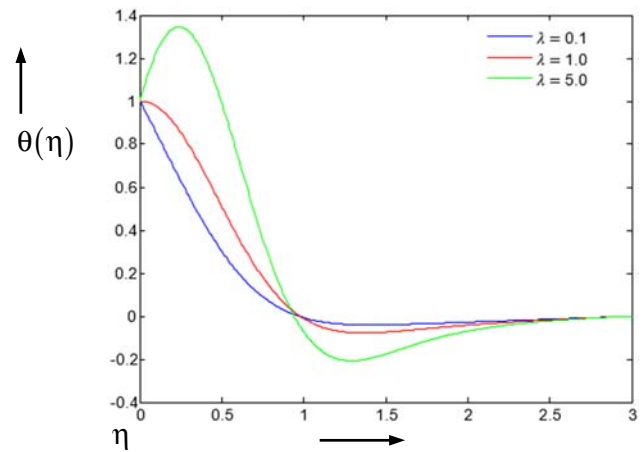Fig.25. Effect of different values of stretching
parameter λ on $f'(\eta)$.

Fig.26. Effect of different values of stretching
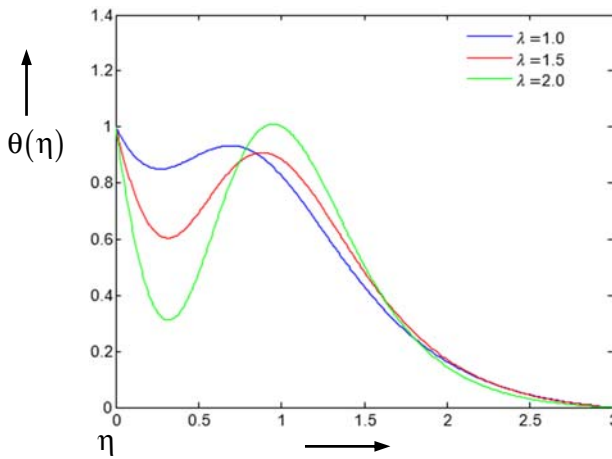parameter λ on $\theta(\eta)$.

Fig.27. Effect of different values of
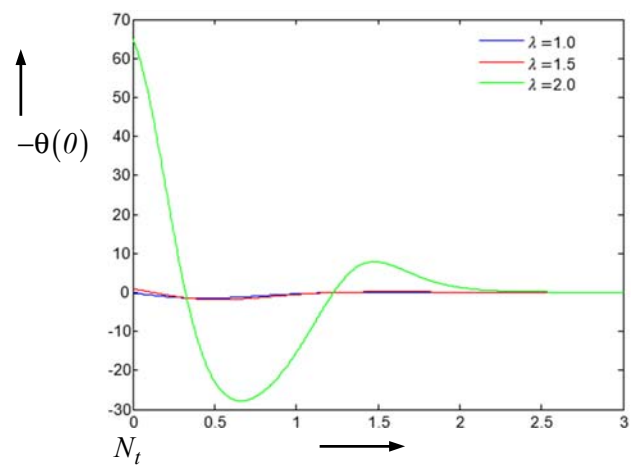stretching parameter λ on $\theta(\eta)$.

Fig.28. Effect of different values of stretching
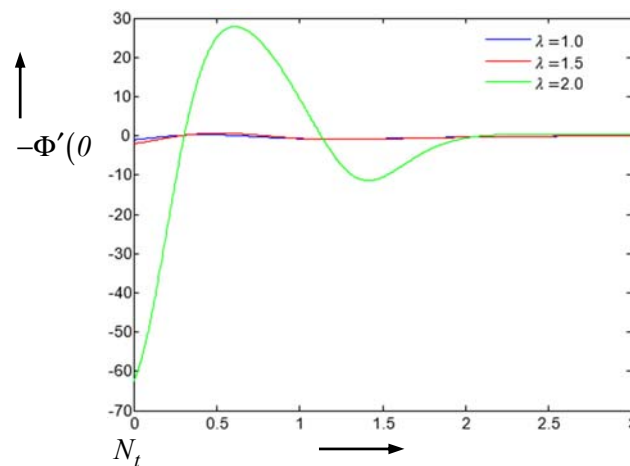parameter λ versus η on $-\theta'(0)$.

Fig.29. Effect of different values of stretching parameter λ on $-\Phi'(0)$.

Figures 30-31 present the effect of the stretching parameter $\lambda < 0$ on the temperature profile and Sherwood number and both profile increase.
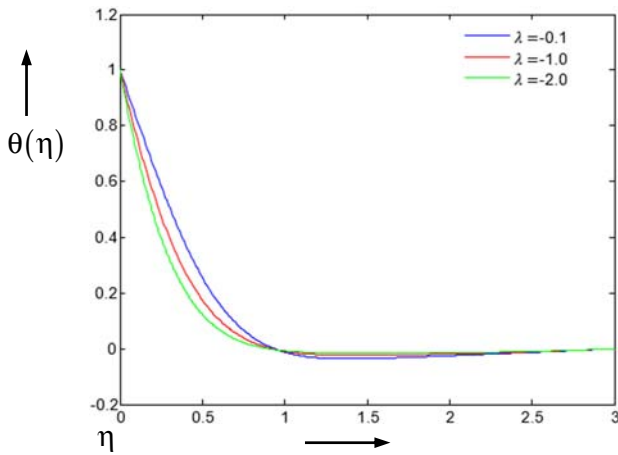

Fig.30. Effect of different values of shrinking parameter $\lambda < 0$ on $\theta(\eta)$.
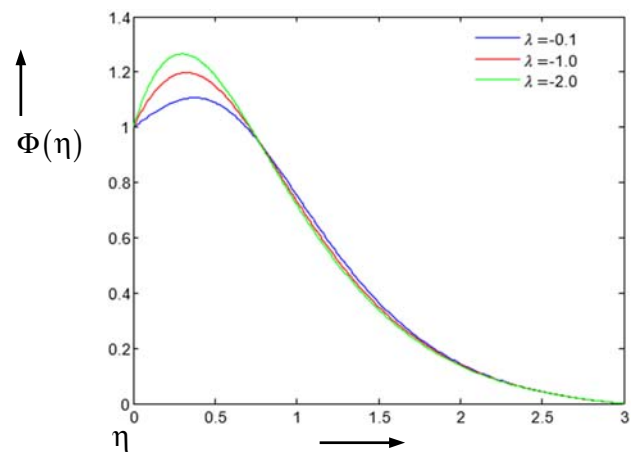
Fig.31. Effect of different values of shrinking parameter $\lambda < 0$ versus η on $\Phi(\eta)$.

Effect of Prandtl number

Figures 32 to 33 present effect of different values of Prandtl number 'Pr' versus η on $f'(\eta)$, $\theta(\eta)$, $\Phi(\eta)$, with $n = 2$, $N_t = 0.1$, $N_b = 0.1$, $Gt = 0.1$, $Gc = 0.1$, $R_d = 0.1$, $Ec = 0.1$, $E = 0.1$, $\lambda = 0.1$, $L_2 = 0.1$.

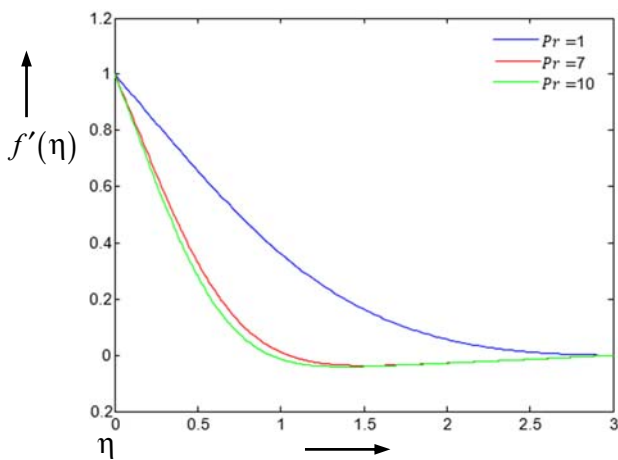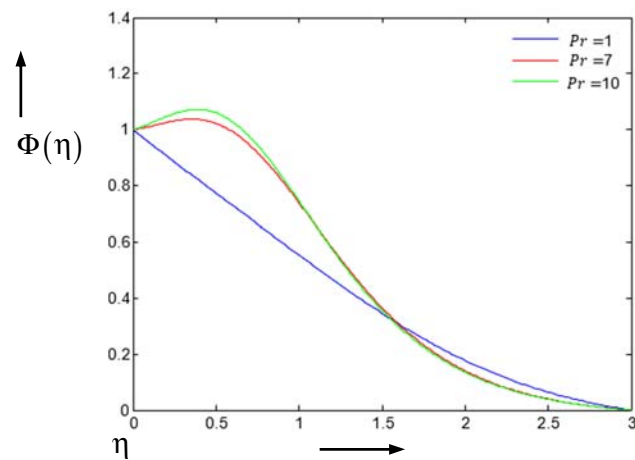Fig.32. Effect of different values of Prandtl number Pr on $f'(\eta)$.

Fig.33. Effect of different values of Prandtl number Pr on $\Phi(\eta)$.

4. Conclusion

1. On increasing the value of the magnetic parameter (M), the velocity and local Nusselt number decrease while the temperature, local Sherwood number, and concentration profile increase. The thermal boundary layer increases with N_t, N_b, and R_d.

2. The mass transfer of the nanofluid flow increases with the increment in the Prandtl number near the wall.
3. The velocity and Sherwood number increase with the increment in the second-order velocity slip parameter. On the other hand, the temperature, concentration profile, and local Nusselt number all decrease.
4. The velocity, temperature, local Nusselt, and Sherwood number of the fluid are found to decrease with the increment in the stretching parameter and the shrinking parameter, temperature profile decrease while the concentration profile increases.
5. The nonlinear parameter *n* causes the fluid's non-dimensional velocity, local Nusselt number, and Sherwood number to increase, while the temperature and concentration profile decrease.

Acknowledgments

Nomenclature

a, c – arbitrary constants

B_0 – magnetic parameter applied along y axis on the flat heated surface

C – concentration of fluid

D_B – Brownian diffusion coefficient

$E = \dfrac{E_0}{\beta_0 U}$ – non-dimensional electric-parameter

$f(\eta)$ – dimensionless stream function

$G_t = \dfrac{A g_x \beta_t}{a^2}$ – non-dimensional thermal free. convection-parameter

$G_c = \dfrac{B g_x \beta_c}{a^2}$ – non-dimensional mass free convection-parameter

g_x – magnitude of the gravity

$M = \dfrac{\sigma B_0^2}{\rho_f a}$ – non-dimensional magnetic-parameter

N_b – Brownian motion parameter

N_t – thermophoresis parameter

Pr – Prandtl number

Re – Reynold's number

T – fluid-temperature

T_w – temperature at the stretching surface

U – fluid velocity of free stream

u, v – velocity in x, y direction

u_w – velocity of the stretching sheet

β_t – thermal expansion coefficient

β_c – mass-diffusion coefficient

σ – electric conductivity which is consider to be constant

α – thermal diffusivity

ν_f – kinematic viscosity of the fluid

ρ_f – fluid density

ρ_p – nanoparticle mass density

$(\rho c)_f$ – heat capacity of the fluid

$(\rho c)_p$ – effective heat capacity of the nanoparticle material

$\tau = \dfrac{(\rho c)_p}{(\rho c)_f}$ – shear stress

Q_0 – heat generation/absorption coefficient

References

[1] Ahmed N., Patel G.S. and Siddappa B. (1990): *Visco-elastic boundary layer flow past a stretching plate and heat transfer.*– Journal of Applied Mathematics and Physics, vol.41, pp.294-298.

[2] Ahmed N. and Khan, N. (2000): *Boundary layer flow past a stretching plate with suction and heat transfer with variable conductivity.*– IJEMS, vol.7, No.1, pp.51-53.

[3] Anderson H.I. (1992): *MHD flow of a viscoelastic fluid past a stretching surface.*– Acta Mechanica, vol.95, pp.227-230.

[4] Bentwhich M. (1978): *Semi-Bounded Slow Viscous Flow Past a Cylinder.* Quarterly Journal of Mechanics and Applied Mathematics, vol.31(4), pp.445-459. https://doi.org/10.1093/qjmam/31.4.445

[5] Chen C.K. and Char M.I. (1988): *Heat transfer of a continuous, stretching surface with suction or blowing.*– Journal of Mathematical Analysis and Application, vol.135, No.2, pp.568-580, https://doi.org/10.1016/0022-247X(88)90172-2.

[6] Choi S.U.S, Zhang Z.G, Yu W. and Lockwood F.E. (2001): *Anomalously thermal conductivity enhancement in nanotube suspensions.*– Appl. Phys. Lett., vol.79, pp.2252-2254, https://doi.org/10.1063/1.1408272.

[7] Cortel R. (2007): *Viscous flow and heat transfer over a nonlinearly stretching sheet.*– Appl. Math Comput., vol.184, No.2, pp.864-873, https://doi.org/10.1016/j.amc.2006.06.077.

[8] Crane L.J. (1970): *Flow past a stretching plate.*– J. Appl. Math. Phys. (ZAMP), vol.21, pp.645-647.

[9] Fang T. and Yao S. Zang J. and Aziz A. (2009): *Slip MHD viscous flow over a stretching-sheet an exact solution.*– Commun. Nonlinear Sci. Numer. Simul., vol.14, pp.3731-3737, https://doi.org/10.1016/j.cnsns.2009.02.012.

[10] Hayat T, Khan WA, Abbas S.Z, and Nadeem S (2020): *Impact of induced magnetic field on second-grade nanofluid flow past a convectively heated stretching sheet.*– Applied Nanoscience, vol.10, pp.3001-3009.

[11] Hsiao K.-L. (2010): *Heat and mass mixed convection for MHD viscoelastic fluid past a stretching sheet with ohmic dissipation.*– Commun. Nonlinear Sci. Numer. Simul., vol.15, pp.1803-1812, http://dx.doi.org/10.1016/j.cnsns.2009.07.006.

[12] Kalidas Das. (2014): *Nanofluid flow over a non-linear permeable stretching sheet with partial slip.*– Journal of the Egyptian Mathematical Society, vol.23, No.2, pp.451-456, https://doi.org/10.1016/j.joems.2014.06.014.

[13] Kang H.U., Kim S.H. and Oh J.M. (2006): *Estimation of thermal conductivity of nanofluid using experimental effective particle volume.*– Exp. Heat Transfer, vol.19, pp.181-191, https://doi.org/10.1080/08916150600619281.

[14] Mahantesh M. Nandeppanavar Abel M.S. and Siddalinappa M.N. (2012): *Second order slip flow and heat transfer over a stretching sheet with non-linear Navier boundary condition.*– International Journal of Thermal Sciences, vol.58, pp.143-150, https://doi.org/10.1016/j.ijthermalsci.2012.02.019.

[15] Nagendramma V. (2017): *Thermo diffusion effects on MHD boundary layer slip flow on nanofluid over a nonlinear stretching sheet through a porous medium.*– Journal of Porous Media, vol.20, No.11, pp.961-970.

[16] Rosca A.V. and Pop I (2013): *Flow and heat transfer over a vertical permeable stretching/shrinking sheet with a second order slip.*– International Journal of Heat and Mass Transfer, vol.60, pp.355-364, https://doi.org/10.1016/j.ijheatmasstransfer.2012.12.028.

[17] Sakiadas B.C. (1961): *Boundary layer equation for two dimensional and axisymmetric flow.*– Journal of American

Institute of Chemical Engineers (AIChE), vol.7, pp.26-28, https://doi.org/10.1155/2013/724385.

[18] Seth G.S. (2019): *Analysis of electromagnetohydrodynamic stagnation point flow of nanofluid over a nonlinear stretching sheet with variable thickness*.– Journal of Mechanics, vol.35, No.5, pp.719-733, https://doi.org/10.1017/jmech.2019.2.

[19] Shen M., Wang F., Chen H. (2015): *MHD mixed convection slip flow near a stagnation-point on a nonlinearly vertical stretching sheet*.– Boundary Value Problems. vol.78, Article Number 2015.78, p.15, DOI 10.1186/s13661-015-0340-6

[20] Siddappa B. and Abel S. (1985): *Non-newtonian flow past a stretching plate*.– Journal of Applied Mathematics and Physics, vol.36, pp.1-3.

[21] Subhas A. and Veena P. (1998): *Visco-elastic fluid flow and heat transfer in a porous medium over a stretching sheet*.– Int. J. Heat and Mass Transfer, vol.33, No.3, pp.531-540.

[22] Khan W.A. and Pop I. (2010).: *Boundary-layer flow of a nanofluid past a stretching sheet*.– Int. J. Heat Mass Transfer, vol.53, pp.2477-2483, https://doi.org/10.1016/j.ijheatmasstransfer.2010.01.032.

[23] Wang C.Y. (1984): *The three-dimensional flow due to a stretching flat surface*.– Phys. Fluids, vol.27, pp.1915-1917, https://doi.org/10.1063/1.864868.